University of Reading

“Pop-on and pop-off” surface chemistry of alanine on Ni{111} under elevated hydrogen pressures

Article

Accepted Version

Nicklin, R. E. J., Shavorskiy, A., Aksoy Akgul, F., Liu, Z., Bennett, R. A. ORCID: https://orcid.org/0000-0001-6266-3510, Sacchi, M. and Held, G. (2018) “Pop-on and pop-off” surface chemistry of alanine on Ni{111} under elevated hydrogen pressures. The Journal of Physical Chemistry C, 122 (14). pp. 7720-7730. ISSN 1932-7447 doi: 10.1021/acs.jpcc.8b00186 Available at https://centaur.reading.ac.uk/77042/

It is advisable to refer to the publisher’s version if you intend to cite from the work. See Guidance on citing.
Published version at: http://dx.doi.org/10.1021/acs.jpcc.8b00186
To link to this article DOI: http://dx.doi.org/10.1021/acs.jpcc.8b00186

Publisher: ACS Publications

All outputs in CentAUR are protected by Intellectual Property Rights law, including copyright law. Copyright and IPR is retained by the creators or other copyright holders. Terms and conditions for use of this material are defined in the End User Agreement.

www.reading.ac.uk/centaur

University of Reading

CentAUR

Central Archive at the University of Reading

Reading's research outputs online

"Pop-on and Pop-off" Surface Chemistry of Alanine on Ni{111} under Elevated Hydrogen Pressures.

Richard E. J. Nicklin,[†,‡] Andrey Shavorskiy,[¶,§] Funda Aksoy Akgul,[¶,‖] Zhi Liu,[¶,⊥] Roger A. Bennett,[†] Marco Sacchi,[#] and Georg Held[*,†,‡]

†*Department of Chemistry, University of Reading, Reading RG6 6AD, UK*

‡*Diamond Light Source Harwell Science and Innovation Campus, Didcot OX11 0QX, UK*

¶*Advanced Light Source, Lawrence Berkeley National Laboratory, Berkeley, CA 94720, USA*

§*MAX IV Laboratory, Lund University, 225 94 Lund, Sweden*

‖*Niğde Ömer Halisdemir University, 51240 Niğde, Turkey*

⊥*ShanghaiTech University, School of Physical Science and Technology, Pudong, Shanghai, 201210, China*

#*Department of Chemistry, University of Surrey, Guildford GU2 7XH, UK*

E-mail: g.held@reading.ac.uk

Phone: +44 (0)118 3786347. Fax: +44 (0)118 3786331

Abstract

The co-adsorption of hydrogen with a simple chiral modifier, alanine, on Ni{111} was studied using Density Functional Theory in combination with ambient-pressure X-ray photoelectron spectroscopy and X-ray absorption spectroscopy at temperatures of 300 K and above, which are representative of chiral hydrogenation reactions. Depending on the hydrogen pressure, the surface enables protons to "pop on and off" the modifier molecules, thus significantly altering the adsorption geometry and chemical nature of alanine from anionic tridentate in ultra-high vacuum to predominantly zwitterionic bidentate at hydrogen pressures above 0.1 Torr. This hydrogen-stabilised modifier geometry allows alternative mechanisms for proton transfer and the creation of enatioselective reaction environments.

Introduction

The chemical state and orientation of amino acids bound to transition metal surfaces are questions of growing interest owing to their relevance to enantioselective catalysis. The best studied enantioselective reaction involving amino acids is the hydrogenation of β-ketoesters (specifically methyl acetoacetate) over amino or hydroxy acid modified Ni catalysts, such as Raney nickel or highly dispersed Ni particles.[1,2] The fact that both activity and selectivity are higher for relatively large catalyst particles suggests that the reaction takes place on low-Miller-index planes.[3,4] Enantioselective hydrogenation of a range of other molecules has also been demonstrated, including β-diketones, methyl ketones and prochiral 2 and 3-alkanones.[5]

A wide variety of techniques and model calculations have been deployed historically to ascertain details regarding the adsorption of amino acids on single crystal transition metal surfaces.[6–28] A consensus has developed that the binding mode for glycine and alanine on Cu is as the anion, with a total of three bonds forming between Cu atoms and the N and O atoms of the adsorbate. This tridentate binding mode is the dominant form on those surface terminations studied, although a minority bidentate mode (where alanine binds as

the zwitterion via the carboxylate O atoms alone) has been seen on Cu{111}.[26] On Ni{111} recent results have shown a more complex picture involving considerable decomposition of the adsorbate, and the relative abundance of the bidentate zwitterion is found to decrease with temperature.[28] Decomposition of the adsorbed molecules on Ni{111} has been observed to begin at ≈ 320 K.

In no case has the effect of hydrogen on the adsorption of amino acids been studied, in spite of the obvious need of H atoms being present at the surface for a Langmuir-Hinshelwood-type hydrogenation reaction. This lack of data has been due to the inability of traditional surface science techniques to operate under the elevated pressure and temperature conditions needed to emulate an active catalyst. Instead experiments tended to be carried out in UHV and at reduced (in some cases cryogenic) temperatures in order to approach surface saturation. This has lead to a "thermodynamic gap" between previous results and the required data. New ambient-pressure instrumentation now makes hydrogen pressures in the range of > 0.1 Torr available for photoemission spectroscopy.[29–31]

In this work we have studied the adsorption and protonation of alanine on Ni{111} in the presence of a hydrogen atmosphere up to 4×10^{-1} Torr in order to determine the effect this will have on the binding mode of the amino acid and its thermal stability. Strikingly, hydrogen was found to "pop onto" the tridentate anion, forming the bidentate zwitterion at high hydrogen pressure ($\geq 1 \times 10^{-1}$ Torr). Partial protonation and/or involvement in hydrogen bonding of the carboxylate group is also seen. When the hydrogen pressure was removed, the proton would "pop off" the amine at 328 K, and the adsorbate reverts to the anionic form. Hydrogen was found to prevent decomposition, with molecular desorption observed for high hydrogen pressures. Hydrogenation of decomposition products is also shown at lower pressures.

Methods

Experimental

XPS (X-ray Photoelectron Spectroscopy) and NEXAFS (Near-Edge X-ray Absorption Fine Structure) experiments were performed at the near-ambient pressure endstation of beamline 9.3.2 at the ALS Synchrotron in Berkeley, USA, which has been described elsewhere.[32,33] The endstation system consisted of two chambers, the high pressure analysis chamber and a UHV preparation chamber, which were linked via a linear transfer system. The base pressures were 1×10^{-8} Torr and 1×10^{-10} Torr in the respective chambers. The preparation chamber housed a LEED system, sputter gun, and a home-built organic evaporator described below. The analysis chamber was attached to the beamline and was equipped to permit XPS at ambient pressures, with a Scienta SES 200 analyzer affording ultimate resolutions between 0.3 eV and 0.6 eV at the energies employed. The analyzer was fitted with electron optics within four differentially pumped stages, each equipped with turbo-molecular pumps. The Ni{111} single crystal (diameter 8 mm) was mounted via tungsten clips to a custom-built cartridge holder containing a button heater (available in both chambers) and linked to a closed cycle cooling loop (when mounted in the analysis chamber) allowing temperatures between 260 K and 1100 K to be used, albeit with a low rate of cooling.

Standard procedures including Ar^+ ion sputtering, and a final annealing step to 1000 K in UHV were applied for sample cleaning. Cleanliness was checked by XPS. The sample temperature was measured by means of a K-type thermocouple pressed against the sample. L-alanine (> 98 % from Aldrich) was dosed by using a home-built evaporator for organic molecules. The evaporator design consists of a resistively heated stainless steel crucible containing a glass tube filled with the organic material to be evaporated. A K-type thermocouple was attached to the crucible for accurate and reproducible temperature control. L-alanine was dosed by heating the crucible to temperatures between 140° C and 155° C.

L-alanine was adsorbed at a sample temperature of 300 K. XP spectra in the C 1s, N 1s,

and O 1s regions were recorded in a geometry close to normal emission using photon energies of 410 eV, 525 eV and 650 eV, respectively, and a pass energy of 50 eV. Spectra of the Fermi edge were measured after each change in the beamline settings with the same monochromator and analyzer parameters (photon energy, pass energy) to calibrate the binding energy offset. In order to study the temperature dependence of the absorbed alanine layers, fast XP spectra were recorded at a photon energy of 650 eV and a rate of typically 42-45 s per spectrum while annealing the sample manually at a rate between 0.1 K s^{-1} and 0.2 K s^{-1} (4-8 K per spectrum).

NEXAFS spectra were recorded in Auger yield mode with the horizontally polarized X-ray beam hitting the sample 15° and 45° with respect to the surface plane (i.e. polarization vector at 15°/45° with respect to the surface normal). The O, C, and N K-edge spectra were recorded with the analyzer set to constant kinetic energies of 507.5 eV, 263.0 eV, 381.0 eV, respectively, and a pass energy of 200 eV, which corresponds to an detection window of approximately ±10 eV centered at the selected kinetic energy. The photon energy was scanned from 525-560 eV (O), 280-310 eV (C), and 395-415 eV (N) in steps of 0.25 eV. The photon flux, I_0, was recorded by measuring the photo-current from a gold mesh inserted into the beamline. NEXAFS spectra were measured for the clean surface and after adsorption of L-alanine. The alanine spectra were normalised with respect to the pre-edge (low photon energy) background, and had the clean-surface spectra subtracted, which were normalised in the same way. In a last step, the background-corrected spectra were divided by I_0 and normalised with respect to the post-edge (high photon energy) background. Note, the photon energy was not calibrated; therefore the peak positions differ slightly from other studies of the same system, e.g. Ref.[28]

Computational - DFT Modelling

Density Functional Theory calculations were performed using the CASTEP code,[34,35] at the generalized gradient approximation level of theory with the Perdew Burke Ernzerhof

exchange-correlation functional.[36] The plane wave basis set was expanded to a 360 eV kinetic energy cutoff and reciprocal space was sampled with a $(3 \times 3 \times 1)$ Monkhorst-Pack k-point grid.[37] Electron-ion interactions were included within the ultrasoft pseudopotential scheme,[38] and van der Waals (vdW) interactions were accounted for with the dispersion force correction methodology developed by Tkatchenko and Scheffler.[39] The force tolerance for the structural calculations was set to 0.04 eV Å^{-1}.

The Ni{111} surface was modelled by a 5 layers thick slab of Ni atoms with a 17 Å vacuum gap and a lateral $p(6 \times 6)$ supercell. Within this supercell different monomer and dimer start geometries were optimised. Here we only report zwitterionic structures compatible with the experimental findings at high hydrogen pressures. A complete account of all modelled structures will be the subject of a forthcoming publication. The adsorption energies for zwitterionic species were calculated as:

$$E_{\text{ads}} = E_{\text{Ala,ads}} - n \cdot E_{\text{Ala,gas}} - E_{\text{clean}} \tag{1}$$

Where $E_{\text{Ala,ads}}$, $E_{\text{Ala,gas}}$, and E_{clean} refer to the total energies of alanine adsorbed on the Ni slab, alanine in the gas phase, and the clean Ni slab; n is 1 for a monomer and 2 for a dimer.

Results and Discussion

Chemical State

Figure 1 shows the effect of increased hydrogen pressure on different coverages of alanine (0.07 ML, 0.19 ML and 0.25 ML). In our earlier study the saturation coverage of alanine on Ni{111} under UHV conditions was determined to be ≈ 0.25 ML.[28] The presence of a hydrogen atmosphere introduces a calibration issue in that inelastic scattering of the ejected photoelectrons by the hydrogen gas causes the spectrum to be attenuated. Removal of the hydrogen pressure, however, causes the signal to recover to the total integrated area prior

to exposure to hydrogen. The spectra presented here are shown with normalised integrated areas. Interestingly, at 2×10^{-3} Torr the loss in intensity of the C 1s and O 1s peaks recorded at photon energies of 410 eV and 650 eV (57 % of the signal measured in UHV) was much more significant than the attenuation of the N 1s peaks recorded with a photon energy of 525 eV (75 %). This is despite the fact that the ejected photoelectrons have approximately the same kinetic energy ($\sim$ 125 eV) and hence the same inelastic mean free path in hydrogen, and that hydrogen absorption of X-rays can be neglected at this pressure. It raises the likelihood that the adsorbate conformation on the surface changes as the hydrogen pressure increases, thus causing variation in photoelectron diffraction intramolecular attenuation, which in turn leads to variation in the relative intensities of C 1, O 1s, and N 1s.

Under UHV conditions the C 1s spectra (Fig. 1 a., b. and c.) exhibit six peaks with binding energies of $\sim$ 283.5 eV, 284.5 eV, 285.0-285.3 eV (this peak is shifting to lower binding energy with increasing alanine coverage), 285.7 eV, 287.3 eV and 288.7 eV. Atomic carbon or H_xCN are assigned at 283.5 eV[40–42] and -C=C- groups at 284.5 eV.[43–49] The 285.3 eV peak's incongruously high intensity at low coverage, coupled with its apparent shift to 285.0 eV at higher coverage, is consistent with known behavior of CO when co-adsorbed with hydrocarbons.[50] Peaks at 285.7 - 286.1 eV, 287.3 eV, and 288.9 - 289.1 eV are assigned as for Cu{110} and Cu{111}.[13,26] The 285.7 eV signal is assigned to the superposition of peaks arising from the methyl and α-C atoms in the anionic alaninate. The 287.3 eV peak is assigned to a combination of the α-C atom of zwitterionic alanine (bound to a -NH_3^+ group) and a decomposition fragment, as in previous work.[28] This interpretation is somewhat challenged by the lack of growth of this peak at high pressures, when the 401.7 eV (-NH_3^+) peak grows (see below). It is suggested that, as the alanine transitions to the bidentate form, the -NH_3^+ group occludes the α-C atom (see NEXAFS and DFT results below) and, hence, the signal generated from this group is attenuated. For the 0.25 ML coverage, as hydrogen pressure is increased above 2×10^{-3} Torr, the spectrum changes significantly with the peak at 287.3 eV being reduced and an apparently new peak growing at 286.5 eV (denoted as "$*$"

in Fig. 1 a.). Concomitantly a sharp peak grows at 288.5 eV (denoted as "$**$" in Figure 1 a.).

Three peaks make up the N 1s spectra, at 401.7 eV, 399.7 eV and 397.3 eV (Fig. 1 d., e., and f.). As in previous work, these peaks are assigned to -NH_3 $^+$, -NH_2, and -CN dissociation fragments, respectively.[24,25,28] Under UHV conditions and at saturation coverage, the N 1s signal at 401.7 eV represents a minority species with an integrated peak area of $\sim$ 10 % relative to the main peak at 399.7 eV. At pressures above 2×10^{-3} Torr this peak shows a significant increase in intensity at the expense of the 399.7 eV species, becoming the dominant peak at 4×10^{-1} Torr.

O 1s spectra (Fig. 1 g., h., and i.) exhibit two chemical environments with peaks at 531.5 eV and 533.5 eV. These environments are assigned to a deprotonated –COO group bound to the surface through both O atoms (531.5 eV) and to a protonated -COOH group, which is presumed to bind to the surface through a single O atom (531.5 eV) leaving the OH (533.5 eV) dangling and available for hydrogen bonds.[24] Alternatively, the 533.5 eV peak could also be assigned to an oxygen atom, which is detached from the surface and acts as hydrogen-bond acceptor of an inter-molecular hydrogen bond, i.e. -COO$\cdots$H. Increasing hydrogen pressure, and so abundance of hydrogen on the surface, increases the intensity of the 533.5 eV peak relative to the 531.5 eV peak from $\sim$ 8 % under UHV conditions and 0.25 ML coverage to $\sim$ 13 % under 4×10^{-1} Torr of hydrogen. There is no such relative growth at lower coverages, which suggests that the -COOH/-COO$\cdots$H groups not only require surface hydrogen to be produced, but also alanine molecules in close proximity. This is presumably because the -COOH groups are stabilised via hydrogen bonding with adjacent alanine molecules.

The changes in the N 1s and O 1s spectra observed at high pressures and saturation coverage support the conclusion that alanine is protonated on the surface at hydrogen pressures above 10^{-1} Torr, with the -NH_2 being converted to -NH_3^+ and, to a lesser extent, -COO to -COOH/-COO$\cdots$H. In both cases the adsorption geometry changes from tridentate to

bidentate and hydrogen attaches to the adsorbate at elevated hydrogen pressures.

As mentioned above, the peak at 286.5 eV grows significantly (marked "$*$" in Fig.1), together with a sharp peak at 288.7 eV (marked "$**$" in Fig. 1). These peaks are unlikely to be due to co-adsorption of a contaminant from the gas phase, as no similar behavior is seen at the lower coverages. Therefore, these peaks are tentatively assigned to the -COOH/-COO$\cdots$H carbon ($*$) and the carbon of the -COO group of the zwitterion still bonded to the surface ($**$) although this has not previously been observed in the UHV data at 250 K.

Molecular Orientation - NEXAFS

NEXAFS data were recorded at 300 K with incidence angles of 45° and 15° with respect to the surface plane, both in UHV and at 4×10^{-1} Torr of hydrogen. The O K-edge spectra are shown in Figure 2. Only these were used for the determination of molecular orientation, as the C data were distorted by carbon contamination of the beamline and the N data showed little angular dependence (see Supporting Information for spectra and more details). The UHV data were acquired at a coverage of 0.21 ML and the hydrogen data at 0.25 ML. The O K-edge spectra contain two main features, at 532.5 eV and around 545 eV. In addition, a low-intensity broad feature around 527.9 eV is observed under hydrogen pressure. This is too low in energy for O K-edge absorption and is probably an artefact due to incomplete background subtraction (note that the clean surface spectra were recorded in UHV). The resonance feature at high photon energy consists of several broad features assigned to a combination of σ resonances arising from C-O, C-C, and C-N bonds. The peak at 532.5 eV is assigned to the π^* transition within the COO group. It shows very different widths and a slight shift in energy between the spectra recorded in UHV (FWHM: 2.5 eV; position: 532.49 eV) and under hydrogen pressure (FWHM: 1,6 eV; position: 532.46 eV). Therefore we associate them with different surface species. The small shoulder at 534.1 eV, which is observed under hydrogen atmosphere, is associated with a π^* transition in the COOH group, which is observed in XPS at these pressures (see Fig. 1). The origin of the different

widths is unclear. It is unlikely that it is inhomogeneous broadening, as XPS indicates a more inhomogeneous layer under hydrogen atmosphere whereas the NEXAFS spectra show a narrower peak. A more likely origin is due to differences in lateral vibrations and/or the electronic overlap between molecular orbitals and metal states on the clean vs hydrogen-covered surface. The angular dependence of the spectra was quantified by fitting with a function composed of a two Gaussian functions representing the π^* resonance and the σ^* resonances, a step function at 534.0 eV, and a linear background (details of data analysis are described in the Supporting Information). The complete fits and the Gaussians representing the π^* resonance peaks at 532.5 eV are included as solid/dashed lines in Figure 2. The intensity ratios between the π^* peaks of the spectra recorded at 45° and 15° are 1.38 for the layer in UHV and 0.64 for 4×10^{-1} Torr hydrogen. These correspond to inclination angles of the COO group of 63° and 34°, respectively, relative to the surface plane.[51] The error margin for these values was estimated as ±5° by applying different methods of data treatment and fitting. The former inclination angle is in good agreement with our earlier investigation of alanine on Ni{111} at 250 K,[28] while the latter is very different from this value.

The conclusion from these NEXAFS data is that the alanine occurs adsorbed on the surface in two different conformations, depending on whether or not the surface is exposed to hydrogen. The conformers are discriminated by differing tilt angles of the –COO plane. It is presumed that these correspond to tridentate (63°) and bidentate (34°) adsorption. It is surprising that the COO plane of the bidentate species appears more titled towards the surface plane than the tridentate species.

Molecular Orientation - DFT

In order to investigate the molecular orientation of the alanine zwitterions further, the adsorption of zwitterion monomers and dimers on Ni{111} was modelled using dispersion-corrected Density Functional Theory. Figure 3 shows the most stable adsorption geometries. The adsorption energies are 1.78 eV for the bidentate monomer (no stable monodentate

monomer structure was found) and 3.49 eV for the most stable dimer, which involves one bidentate and one monodentate molecule. This is in good agreement with previously reported vdW-corrected DFT results for amino acids adsorbed on metal surfaces.[52] The dimer is a model of the adsorbate at high coverage and allows investigating the effect of hydrogen bonding interactions. Its structure indicates strong hydrogen bonds between neighboring molecules through the -NH_3^+ and the COO^- groups with an O$\cdots$H distance of 1.67 Å. A weaker intra-molecular hydrogen bond is observed between the -NH_3^+ and the COO^- groups in the monomer, where the O$\cdots$H distance is 1.90 Å. However no such intra-molecular hydrogen bonding is observed in the dimer, where the corresponding O$\cdots$H distances are greater than 2.2 Å, which is too large for a significant interaction.[53] In addition, there appears to be significant (electrostatic) interaction between one H atom of each of the -NH_3^+ groups and the Ni substrate (Ni-H distances 2.36/2.42 Å in the dimer and 2.50/2.56 Å in the monomer), which explains the small tilt angles of the COO groups. The tilt angles (with respect to the surface plane) of the geometries shown in Figure 3 are 33.5° for the monomer and 34.6°/41.0° for the dimer. This is in good agreement with the experimental value of 34° from NEXAFS. Interestingly, the surface bond of the two carboxylate groups in the dimer is not equivalent. One of the oxygen atoms of the molecule on the right in Figure 3 is significantly lifted in order to accommodate the hydrogen bond with the neighboring molecule. This is compatible with the observation of the O 1s peak at 533.5 eV in XPS (see Fig. 1), which was assigned to an oxygen atom involved in an inter-molecular hydrogen bond. Similar "μ_2" transitions in high coverage phases of alanine have been hypothesized to occur on other metal surfaces.[27] The contribution of the hydrogen bond to the adsorption energy was estimated at 0.60 eV by calculating the energies for the two component molecules separately. Nevertheless, the dimer appears slightly less stable than the bidentate monomer (1.74 eV vs 1.78 eV per molecule).

Tridentate monomer and dimer structures of anionic alanine were also modelled by DFT (see Supporting Information). The COO tilt angles of the most stable structures range between 28.6° and 33.1°, which deviates significantly from the experimental value of 63°

found by NEXAFS.

Temperature Dependence

The influence of hydrogen on the decomposition pathway was probed using Temperature Programmed XPS (TP-XPS). The decomposition of organic adsorbates on metal surfaces in vacuum is normally considered in terms of sequential dehydrogenation reactions.[54] Under elevated hydrogen pressures it might be expected that the chemical equilibrium is shifted towards the preservation of the intact adsorbate up to higher temperatures. This is, however, not observed.

N 1s TPXPS data for hydrogen pressures of 2×10^{-3} Torr, 1×10^{-1} Torr, and 4×10^{-1} Torr are presented in Figures 4 a.-c., with line profiles integrated over a width of 2 eV being shown in Figures 4 d.-f.. In all cases 0.25 ML of alanine were deposited at 300 K in UHV and afterwards exposed to the indicated pressures.

The 399.7 eV peak (-NH_2) begins to decrease at $\sim$ 328 K in all the systems probed while the 401.7 eV (-NH_3^+) peak decreases from the start of the temperature ramp at 300 K. In each case, the -NH_3^+ and -NH_2 peak intensities drop to near zero by 400 K, while the 397.3 eV peak (associated with CN fragments) grows. The decay and loss of these peaks are taken as a proxy for the thermal decomposition of the amino acid on the surface, and show that this decomposition process is not significantly inhibited at these hydrogen pressures. At pressures of 2×10^{-3} Torr and 1×10^{-1} Torr, the 399.7 eV peak shifts to 400.0 eV above $\sim$ 350 K, which is evidence that the amine group decomposes at this temperature.

The behavior is very different at 4×10^{-1} Torr hydrogen. Figures 4 c. and f. only show diminution with increasing temperature in the intensities of the peaks associated with anionic (up to 328 K) and zwitterionic alanine (up to $\sim$ 400 K). There is no growth of the -CN fragment at 397.3 eV. This can be explained either by the bidentate form desorbing molecularly, or by decomposition of the bidentate amino acid followed by a rapid "clean up" reaction.

It is evident from Figure 4 that, under increased hydrogen pressure, the ultimately evolved CN species is lost from the surface at progressively lower temperatures: at 730 K under UHV conditions[28] (813 K in Figure 5 under UHV with different preparation), at 660 K for 2×10^{-3} Torr, 640 K for 1×10^{-1} Torr, and not evolving at all for 4×10^{-1} Torr. This is presumably through hydrogenation to an H_xCN species. Similar behavior has been observed for the hydrogenation of cyclohexamine residues on Ni{111} and {100}.[55]

Figure 5 shows TP-XPS data for a saturated alanine layer exposed to 4×10^{-1} Torr at 300 K hydrogen before being returned to UHV conditions at the same temperature. Initially, the protonation is not reversed, however, the C 1s and N 1s spectra indicate a conversion back to the anionic species at approximately 320 K. Intensity is lost from the 401.7 eV N 1s peak, while the 399.7 eV peak grows by a similar amount. This is consistent with a switch from the zwitterionic bidentate form to tridentate anionic alanine, normally seen under UHV conditions (see Fig. 1). The proton detaches from the amine group prior to the decomposition of the body of the adsorbate molecule. The ensuing decomposition follows the process discussed previously for the layer prepared under UHV conditions.[28]

Conclusions and Summary

Under elevated hydrogen pressures ($> 1 \times 10^{-1}$ Torr), XPS and NEXAFS data concur that the amino group of the adsorbed alanine is protonated and converts from anionic -NH_2 to a zwitterionic -NH_3^+ species. As a result alanine re-orients on the surface. The majority species in the hydrogen atmosphere has a bidentate binding mode with the -NH_3^+ group detached from the surface, as opposed to a tridentate binding mode under UHV conditions, where the -NH_2 group forms an additional bond with the surface. It is important to note, however, that this transition is only observed at saturation coverage, 0.25 ML. The layers with lower coverages, 0.19 ML and 0.07 ML, investigated in this study remain in a tridentate configuration up to the maximum pressure of 4×10^{-1} mbar.

This alteration to the binding mode raises some intriguing possibilities: First, it has generally been assumed hitherto that the source of hydrogen for the enantioselective hydrogenation of target molecules was dissociated hydrogen on the metal surface.[5,56–60] The protonation of the modifier molecule alanine offers the alternative possibility that a proton is taken from the -NH_3^+ group as at least one step in the hydrogenation of the target molecule. Such reaction steps are known from natural enzyme reactions.[61] Second, breaking the bond of the amine group with the surface at elevated hydrogen pressures alters the alanine adsorption complex from tridentate to bidentate binding. This transition removes the "chiral footprint".[62] Consequently one could argue that a chiral interaction on the surface between a single modifier molecule and the target molecule can no longer be the source of the enantioselectivity. It is more likely that the enantioselective reaction environment is created by a supra-molecular arrangement involving several modifier molecules. Also the small tilt angle of the COO group with respect to the surface plane hints at structures affected by strong hydrogen bonding, which is supported by our DFT modelling. The dimer structure shown on the right-hand side of Figure 3 shows hydrogen bonds between neighboring molecules and a hydrogen-mediated attractive interaction between the -NH_3^+ groups and the surface, which both contribute to the small tilt angles of the carboxylate groups. In addition, the dimer in Figure 3 clearly provides a chiral template for adsorbed reactants and the -NH_3^+ groups of both zwitterions can act as hydrogen source for the hydrogenation reaction. Of course, there is a multitude of other possible arrangements, including higher oligomers and compounds of zwitterions and anions, such as those found on Pd{111},[63,64] which may be compatible with the experimental findings (note that there is still a significant amount of anionic alanine present on the surface at 4×10^{-1} Torr). However, they will most likely share the above features of hydrogen bonding and chiral templating.

There is a significant mismatch between the experimental value for the tilt angle of the COO group in the anionic species found under UHV conditions (63°) and the values found by DFT modelling for the most stable monomer and dimer structures (around 30°). This

may again point towards more complicated supra-molecular structures.

Our TP-XPS experiments examined the thermal stability of protonated alanine. Under the maximum hydrogen pressure of 4×10^{-1} Torr of this study the bidentate zwitterionic and tridentate anionic forms desorb molecularly. Under these conditions thermal decomposition on the surface is not observed in contrast to previously reported behavior in UHV. At the intermediate pressures examined (1×10^{-3} Torr and 1×10^{-1} Torr) the -CN decomposition fragments, which are generated by thermal cracking of the alanine, are hydrogenated and leave the surface at far lower temperatures than in UHV (where the -CN fragment releases N_2 and dissolves C into the bulk).

Protonation of alanine followed by the removal of the applied hydrogen pressure results in a meta-stable bidentate protonated species on the surface, which converts back to the tridentate anionic form at 320 K before decomposing following the same path as in UHV (see Fig. 5). Our experimental set-up did not allow monitoring the evolution of hydrogen during the temperature ramp, but earlier work has shown that hydrogen desorbs from Ni{111} in the temperature range between 300 K and 400 K under UHV conditions.[65,66] It is, therefore, not unlikely that the transition from zwitterionic bidentate to tridentate anionic alanine is triggered by the desorption of co-adsorbed hydrogen from the surface, thus making adsorption sites available for the de-protonation reaction. As surface hydrogen cannot be detected by XPS, it impossible to estimate the amount of hydrogen present at the surface under elevated pressure conditions. It is, however, obvious from the TP-XPS data shown in Figure 4 that significant levels of surface hydrogen are present well above 400 K to affect the reaction pathway of the decomposition products.

In summary, co-adsorption of the simplest molecule (H_2) with the simplest chiral modifier (alanine) at temperatures representative of chiral hydrogenation reactions ($\gtrsim$ 300 K)[1] has been found to significantly alter the chemical environment on a model catalyst surface. This study re-emphasises the need for care when extending conclusions formed in UHV and low temperatures across the thermodynamic gap to room temperature reactions. This behavior

further shows that more surface-sensitive experiments under near-reaction conditions (e.g. interaction with solvents, oxide layers and other reagents) are needed to gain understanding of complex multi-adsorbate systems.

Supporting Information Available

The following files are available free of charge.

- `Ni111_Ala_H2_SI_rev.pdf`: details of NEXAFS data analysis; additional NEXAFS spectra (C K-edge, N K-edge); DFT structures of anionic alanine.
- `Ni111-6x6_5l_3fix-Zv.xyz`: complete set of coordinates for the DFT model of the monomer adsorption complex.
- `Ni111-6x6_5l_3fix-ZZv.xyz`: complete set of coordinates for the DFT model of the dimer adsorption complex.

Acknowledgement

The research leading to these results has received funding from the UK's EPSRC through grants EP/G068593/1 and EP/H015493/1. M.S. acknowledges the Royal Society for funding his fellowship and the HEC Materials Chemistry Consortium, which is funded by EPSRC (EP/L000202), for use of the ARCHER UK National Supercomputing Service. The authors also thank the staff of ALS for their help during the experiments.

References

(1) Izumi, Y. Modified Raney nickel (MRNi) catalyst: Heterogeneous enantiodifferentiating (asymmetric) catalyst. *Adv. Catal.* **1983**, *32*, 215–271.

(2) Keane, M. A. Interaction of optically active tartaric acid with a nickel-silica catalyst: Role of both the modification and reaction media in determining enantioselectivity. *Langmuir* **1997**, *13*, 41–50.

(3) Nitta, Y.; Sekine, F.; Imanaka, T.; Teranishi, S. The effect of crystallite size of nickel on the enantioselectivity of modified nickel catalysts. *Bull. Chem. Soc. Jpn.* **1981**, *54*, 980–984.

(4) Wolfson, A.; Geresh, S.; Landau, M. V.; M. Herskowitz, M. Enantioselective hydrogenation of methyl acetoacetate catalyzed by nickel supported on activated carbon or graphite. *Appl. Catal. A* **2001**, *208*, 91–98.

(5) Baiker, A. Progress in asymmetric heterogeneous catalysis: Design of novel chirally modified platinum metal catalysts. *J. Mol. Catal. A* **1997**, *115*, 473.

(6) Inoue, Y.; Okabe, K.; Yasumori, I. X-ray photoelectron spectra of adsorbed methyl acetoacetate and coordinated tartaric acid, aspartic acid and alanine on the nickel surface. *Bull. Chem. Soc. Jpn.* **1981**, *54*, 613–614.

(7) Barlow, S. M.; Raval, R. Complex organic molecules at metal surfaces: bonding, organisation and chirality. *Surf. Sci. Rep.* **2003**, *50*, 201–341.

(8) Baddeley, C. J.; Jones, T. E.; Trant, A. G.; Wilson, K. E. Fundamental investigations of enantioselective heterogeneous catalysis. *Top. Catal.* **2011**, *54*, 1348–1356.

(9) Ernst, K.-H. Amplification of chirality in two-dimensional molecular lattices. *Current Opinion in Colloid and Interface Science* **2008**, *13*, 54–59.

(10) Ernst, K.-H. Molecular chirality at surfaces. *Phys. Status Solidi B* **2012**, *249*, 2057–2088.

(11) Barlow, S. M.; Louafi, S.; Le Roux, D.; Williams, J.; Muryn, C.; Haq, S.; Raval, R. Polymorphism in supramolecular chiral structures of R- and S-alanine on Cu(110). *Surf. Sci.* **2005**, *590*, 243–263.

(12) Hasselström, J.; Karis, O.; Weinelt, M.; Wassdahl, N.; Nilsson, A.; Nyberg, M.; Pettersson, L. G. M.; Samant, M. G.; Stöhr, J. The adsorption structure of glycine adsorbed on Cu(110); comparison with formate and acetate/Cu(110). *Surf. Sci.* **1998**, *407*, 221–236.

(13) Jones, G.; Jones, L. B.; Thibault–Starzyk, F.; Seddon, E. A.; Raval, R.; Jenkins, S. J.; Held, G. The local adsorption geometry and electronic structure of alanine on Cu110. *Surf. Sci.* **2006**, *600*, 1924–1935.

(14) Jones, T. E.; Baddeley, C. J.; Gerbi, A.; Savio, L.; Rocca, M.; Vattuone, L. Molecular ordering and adsorbate induced faceting in the Ag110-(S)-glutamic acid system. *Langmuir* **2005**, *21*, 9468–9475.

(15) Jones, T. E.; Urquhart, M. E.; Baddeley, C. J. An investigation of the influence of temperature on the adsorption of the chiral modifier, (S)-glutamic acid, on Ni111. *Surf. Sci.* **2005**, *587*, 69–77.

(16) Gladys, M. J.; Stevens, A. V.; Scott, N. R.; Jones, G.; Batchelor, D.; Held, G. Enantiospecific adsorption of alanine on the chiral Cu(531) surface. *J. Phys. Chem. C* **2007**, *111*, 8331–8336.

(17) Thomsen, L.; Tadich, A.; Riley, D. P.; Cowie, B. C. C.; Gladys, M. J. Investigating the enantioselectivity of alanine on a chiral Cu{421}(R) surface. *J. Phys. Chem. C* **2012**, *116*, 9472–9480.

(18) Thomsen, L.; Wharmby, M.; Riley, D. P.; Held, G.; Gladys, M. J. The adsorption and stability of sulfur containing amino acids on Cu531. *Surf. Sci.* **2009**, *603*, 1253 – 1261.

(19) Schiffrin, A.; Riemann, A.; Auwärter, W.; Pennec, Y.; Weber-Bargioni, A.; Cvetko, D.; Cossaro, A.; Morgante, A.; Barth, J. V. Zwitterionic self-assembly of L-methionine nanogratings on the Ag(111) surface. *PNAS* **2007**, *104*, 5279–5284.

(20) Eralp, T.; Zheleva, Z. V.; Shavorskiy, A.; Dhanak, V. R.; Held, G. Adsorption geometry of glycine on the intrinsically chiral Cu531 Surface. *Langmuir* **2010**, *26*, 10918–10923.

(21) Eralp, T.; Shavorskiy, A.; Zheleva, Z. V.; Held, G.; Kalashnyk, N.; Ning, Y.; Linderoth, T. R. Global and local chiral resolution of serine on the Cu{110} surface. *Langmuir* **2010**, *26*, 18841–18851.

(22) Clegg, M. L.; Morales de la Garza, L.; Karakatsani, S.; King, D. A.; Driver, S. M. Chirality in amino acid overlayers on Cu surfaces. *Top. Catal.* **2011**, *54*, 1429–1444.

(23) Eralp, T.; Cornish, A.; Shavorskiy, A.; Held, G. The study of chiral adsorption systems using synchrotron-based structural and spectroscopic techniques: Stereospecific adsorption of serine on Au-modified chiral Cu531 surfaces. *Top. Catal.* **2011**, *54*, 1414–1428.

(24) Shavorskiy, A.; Eralp, T.; Schulte, K.; Bluhm, H.; Held, G. Surface chemistry of glycine on Pt111 in different aqueous environments. *Surf. Sci.* **2013**, *607*, 10–19.

(25) Shavorskiy, A.; Aksoy, F.; Grass, M. E.; Liu, Z.; Bluhm, H.; Held, G. A Step toward the wet surface chemistry of glycine and alanine on Cu{110}: Destabilization and decomposition in the presence of near-ambient water vapor. *J. Am. Chem. Soc.* **2011**, *133*, 6659–6667.

(26) Baldanza, S.; Cornish, A.; Nicklin, R. E.; Zheleva, Z. V.; Held, G. Surface chemistry of alanine on Cu111: Adsorption geometry and temperature dependence. *Surf. Sci.* **2014**, *629*, 114–122.

(27) Madden, D. C.; Temprano, I.; Sacchi, M.; Blanco-Rey, M.; Jenkins, S. J. Self-organized overlayers formed by alanine on Cu{311} surfaces. *J. Phys. Chem. C* **2014**, *118*, 18589–18603.

(28) Nicklin, R. E. J.; Cornish, A.; Shavorskiy, A.; Baldanza, S.; Schulte, K.; Liu, Z.; Bennett, R. A.; Held, G. Surface chemistry of alanine on Ni{111}. *J. Phys. Chem.* **2015**, *119*, 26566–26574.

(29) Ogletree, D. F.; Bluhm, H.; Lebedev, G.; Fadley, C. S.; Hussain, Z.; Salmeron, M. A differentially pumped electrostatic lens system for photoemission studies in the millibar range. *Rev. Sci. Instr.* **2002**, *73*, 3872.

(30) Bluhm, H.; Andersson, K.; Araki, T.; Benzerara, K.; Brown, G.; Dynes, J.; Ghosal, S.; Gilles, M.; Hansen, H.-C.; Hemminger, J. et al. Soft X-ray microscopy and spectroscopy at the molecular environmental science beamline at the Advanced Light Source. *J. Electron. Spectrosc. Relat. Phenom.* **2006**, *150*, 86.

(31) Bluhm, H. Photoelectron spectroscopy of surfaces under humid condition. *J. Electron. Spectrosc. Relat. Phenom.* **2010**, *177*, 71–84.

(32) Nyholm, R.; Andersen, J. N.; Johansson, U.; Jensen, B. N.; Lindau, I. Beamline I311 at MAX-LAB: a VUV/soft X-ray undulator beamline for high resolution electron spectroscopy. *Nucl. Instr. Methods Phys. Res. Sect A* **2001**, *467*, 520–524.

(33) Grass, M. E.; Karlsson, P. G.; Aksoy, F.; Lundqvist, M.; Wannberg, B.; Mun, B. S.; Hussain, Z.; Liu, Z. New ambient pressure photoemission endstation at Advanced Light Source beamline 9.3.2. *Rev. Sci. Instrum.* **2010**, *81*, 053106–1–7.

(34) Segall, M. D.; Lindan, P. J. D.; Probert, M. J.; Pickard, C. J.; Hasnip, P. J.; Clark, S. J.; Payne, M. C. First-principles simulation: ideas, illustrations and the CASTEP code. *J. Phys.: Condens. Matter* **2002**, *14*, 2717–2744.

(35) Clark, S. J.; Segall, M. D.; Pickard, C. J.; Hasnip, P. J.; Probert, M. J.; Refson, K.; Payne, M. C. First principles methods using CASTEP. *Z. Kristallogr.* **2005**, *220*, 567–570.

(36) Perdew, J. P.; Burke, K.; Ernzerhof, M. Generalized gradient approximation made simple. *Phys. Rev. Lett.* **1997**, *78*, 1396.

(37) Monkhorst, H. J.; Pack, J. D. Special points for Brillouin-zone integrations. *Phys. Rev. B* **1976**, *13*, 5188–5192.

(38) Vanderbilt, D. Soft self-consistent pseudopotentials in a generalized eigenvalue formalism. *Phys. Rev. B* **1990**, *41*, 7892–7895.

(39) Tkatchenko, A.; Scheffler, M. Accurate molecular Van der Waals interactions from ground-state electron density and free-atom reference data. *Phys. Rev. Lett.* **2009**, *102*, 073005,1–4.

(40) Carley, A. F.; Chinn, M.; Parkinson, C. R. The adsorption and oxidation of cyanogen on copper surfaces. *Surf. Sci.* **2003**, *537*, 64–74.

(41) Carley, A. F.; Chinn, M.; Parkinson, C. R. Polymerisation of cyanogen on graphite and copper films. *Surf. Sci. Lett.* **2002**, *517*, L563–L567.

(42) Fleming, G.; Adib, K.; Rodriguez, J.; Barteau, M.; White, J.; Idriss, H. The adsorption and reactions of the amino acid proline on rutile TiO2(1;1;0) surfaces. *Surf. Sci.* **2008**, *602*, 2029–2038.

(43) Lorenz, M.; Fuhrmann, T.; Streber, R.; Bayer, A.; Bebensee, F.; Gotterbarm, K.; Kinne, M.; Traenkenschuh, B.; Zhu, J. F.; Papp, C. et al. Ethene adsorption and dehydrogenation on clean and oxygen precovered Ni(111) studied by high resolution x-ray photoelectron spectroscopy. *J. Chem. Phys.* **2010**, *133*, 014706.

(44) Papp, C.; Denecke, R.; Steinrück, H.-P. Adsorption and reaction of cyclohexene on a Ni(111) surface. *Langmuir* **2007**, *23*, 5541–5547.

(45) Papp, C.; Fuhrmann, T.; Tränkenschuh, B.; Denecke, R.; Steinrück, H.-P. Kinetic isotope effects and reaction intermediates in the decomposition of methyl on flat and stepped platinum (111) surfaces. *Chem. Phys. Lett* **2007**, *442*, 176–181.

(46) Steinrück, H.-P.; Fuhrmann, T.; Papp, C.; Traenkenschuh, B.; Denecke, R. A detailed analysis of vibrational excitations in X-ray photoelectron spectra of adsorbed small hydrocarbons. *J. Chem. Phys.* **2006**, *125*, 204706–1–8.

(47) Zhao, Q.; Deng, R.; Zaera, F. Thermal activation and reaction of allyl alcohol on Ni(100). *Surf. Sci.* **2011**, *605*, 1236–1242.

(48) Zhao, Q.; Deng, R.; Zaera, F. Formation of an oxametallacycle surface intermediate via thermal activation of 1-chloro-2-methyl-2-propanol on Ni(100). *J. Phys. Chem. C* **2010**, *114*, 7913–7919.

(49) Castonguay, M.; Roy, J.-R.; McBreen, P. H. Sequential selective formation of adsorbed tert-butoxy and tert-butyl groups from tert-butyl formate on Ni(111). *Langmuir* **2000**, *16*, 8306–8310.

(50) Held, G.; Schuler, J.; Sklarek, W.; Steinrück, H.-P. Determination of adsorption sites of pure and coadsorbed CO on Ni(111) by high resolution X-ray photoelectron spectroscopy. *Surf. Sci.* **1998**, *398*, 154–171.

(51) Stöhr, J.; Outka, D. A. Determination of molecular orientations on surfaces from the angular dependence of near-edge x-ray-absorption fine-structure spectra. *Phys. Rev. B* **1987**, *36*, 7891–7901.

(52) Sacchi, M.; Jenkins, S. J. Co-adsorption of water and glycine on Cu{110}. *Phys.Chem.Chem.Phys.* **2014**, *16*, 6101–6107.

(53) Jones, G.; Jenkins, S. J.; King, D. A. Hydrogen bonds at metal surfaces: Universal scaling and quantification of substrate effects. *Surf. Sci.* **2006**, *600*, L224–L228.

(54) Bent, B. E. Mimicking aspects of heterogeneous catalysis:? Generating, isolating, and reacting proposed surface intermediates on single crystals in vacuum. *Chemical Reviews* **1996**, *96*, 1361–1390.

(55) Huang, S.; Fisher, D. A.; Gland, J. In situ studies of cyclohexylamine dehydrogenation and hydrogenation on the Ni(111) Surface. *J. Phys. Chem.* **1996**, *100*, 13629–13635.

(56) Baddeley, C. J. Fundamental investigations of enantioselective heterogeneous catalysis. *Top. Catal.* **2003**, *25*, 17–28.

(57) Baiker, A. Transition state analogues - a guide for the rational design of enantioselective heterogeneous hydrogenation catalysts. *J. Mol. Catal. A* **2000**, *163*, 205.

(58) Baiker, A. Reflections on chiral metal surfaces and their potential for catalysis. *Catal. Today* **2005**, *100*, 159–170.

(59) Osawa, T.; Harada, T.; Tai, A. Enantio-differentiating hydrogenation of prochiral ketones over modified nickel. *Catalysis Today* **1997**, *37*, 465–840.

(60) Kyriakou, G.; Beaumont, S. K.; Lambert, R. M. Aspects of heterogeneous enantioselective catalysis by metals. *Langmuir* **2011**, *27*, 9687–9695.

(61) Antonyuk, S. V.; Strange, R. W.; Ellis, M. J.; Bessho, Y.; Kuramitsu, S.; Inoue, Y.; Yokoyama, S.; Hasnaina, S. S. Structure of D-lactate dehydrogenase from aquifex aeolicus complexed with NAD+ and lactic acid (or pyruvate). *Acta Cryst F* **2009**, *65*, T209–T213.

(62) Humblot, V.; Haq, S.; Muryn, C.; Hofer, W. A.; Raval, R. From local adsorption stresses to chiral surfaces: (R,R)-tartaric acid on Ni(110). *J. Am. Chem. Soc.* **2002**, *124*, 503–510.

(63) Mahapatra, M.; Burkholder, L.; Bai, Y.; Garvey, M.; Boscoboinik, J. A.; Hirschmugl, C.; Tysoe, W. T. Formation of chiral self-assembled structures of amino acids on transition-metal surfaces: Alanine on Pd (111). *J. Phys. Chem. C* **2014**, *118*, 6856–6865.

(64) Mahapatra, M.; Burkholder, L.; Devarajan, S. P.; Boscoboinik, A.; Garvey, M.; Bai, Y.; Tysoe, W. T. Formation of induced-fit chiral templates by amino acid-functionalized Pd(111) surfaces. *J. Phys. Chem. C* **2015**, *119*, 3556–3563.

(65) Christmann, K.; Schober, O.; Ertl, G.; Neumann, M. Adsorption of hydrogen on nickel single crystal syrfaces. *J. Chem. Phys.* **1974**, *60*, 4528–4540.

(66) Braun, W.; Steinrück, H.-P.; Held, G. The surface geometry of carbonmonoxide and hydrogen co-adsorbed on Ni{111}. *Surf. Sci.* **2005**, *574*, 193–204.

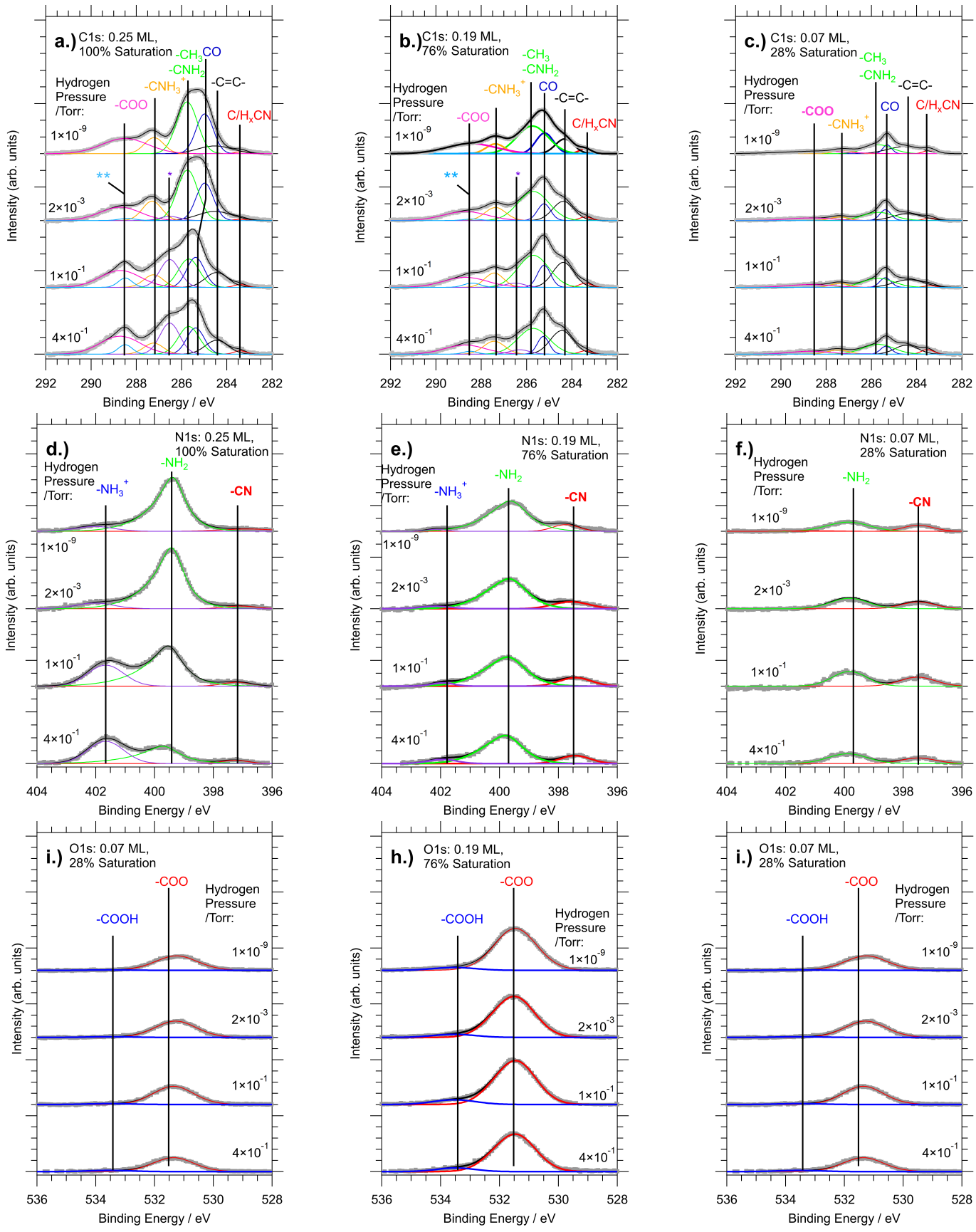
a.) C1s: 0.25 ML, 100% Saturation
b.) C1s: 0.19 ML, 76% Saturation
c.) C1s: 0.07 ML, 28% Saturation
d.) N1s: 0.25 ML, 100% Saturation
e.) N1s: 0.19 ML, 76% Saturation
f.) N1s: 0.07 ML, 28% Saturation
i.) O1s: 0.07 ML, 28% Saturation
h.) O1s: 0.19 ML, 76% Saturation
i.) O1s: 0.07 ML, 28% Saturation
Hydrogen Pressure /Torr:
-COO
-CNH3+
-CH3
-CNH2
CO
-C=C-
C/HxCN
-NH3+
-NH2
-CN
-COOH
1×10-9
2×10-3
1×10-1
4×10-1
**
*
Intensity (arb. units)
Binding Energy / eV

Figure 1: C 1s (a.-c.), N 1s (d.-f.) and O 1s (g.-i.) XP spectra of L-alanine layers on Ni{111} of different coverages under hydrogen pressures varying from UHV to 4×10^{-1} Torr. All spectra were recorded at 300 K, with photon energies of 410 eV, 525 eV and 650 eV, respectively. Grey dots represent raw data and continuous lines fitted peaks.

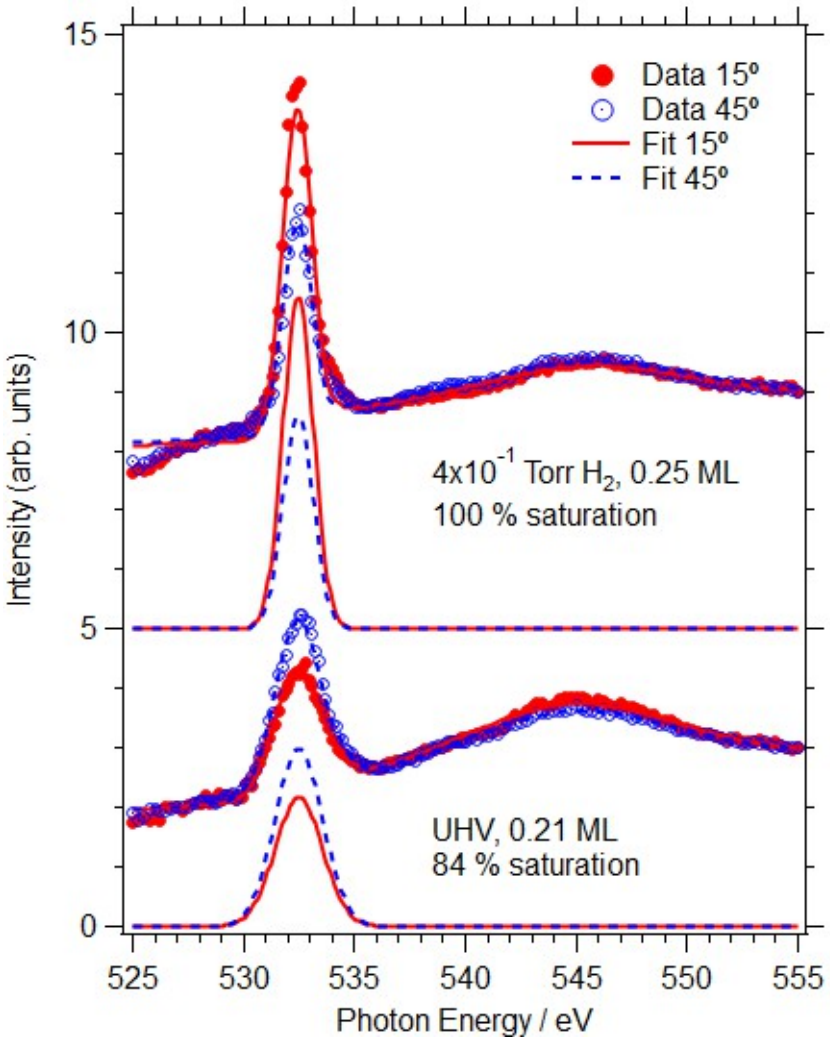

Figure 2: Auger yield O K-edge NEXAFS for alanine adsorbed on Ni{111} at 300 K. Spectra recorded in UHV (0.21 ML, bottom) and 4×10^{-1} Torr hydrogen (0.25 ML, top) at angles of incidence of 15° (full circles/solid lines) and 45° (open circles/dotted lines) with respect to the surface plane. Dots represent data points; the lines overlapping with the data points represent the complete fits to the spectra, as discussed in the text; the lines below the actual spectra represent the π^* resonance peaks extracted from the fits.

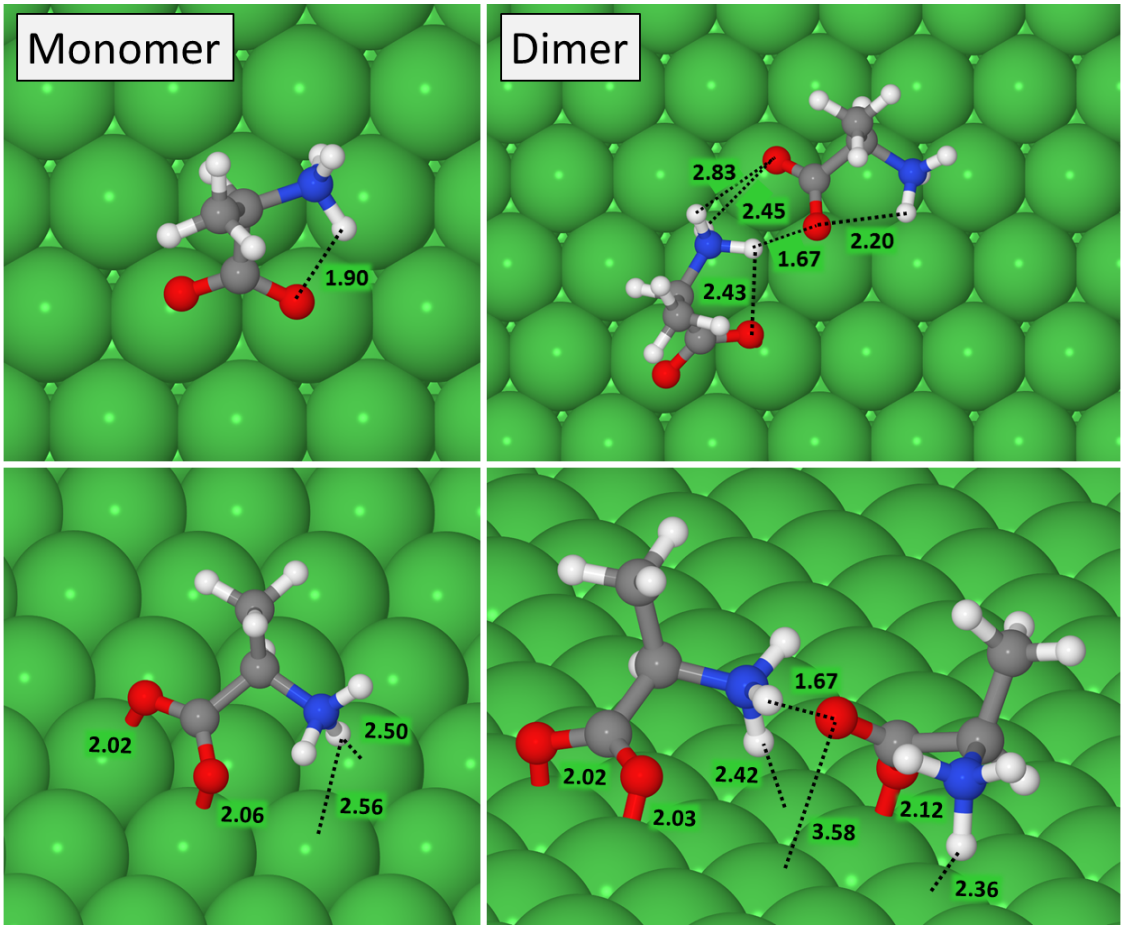

Figure 3: DFT-optimised adsorption geometry of an isolated alanine zwitterion (left) and a dimer of alanine zwitterions (right) on Ni{111}. The top row shows top views, the bottom row side views of the same geometries. Key bond lengths are indicated the diagrams (see text for details).

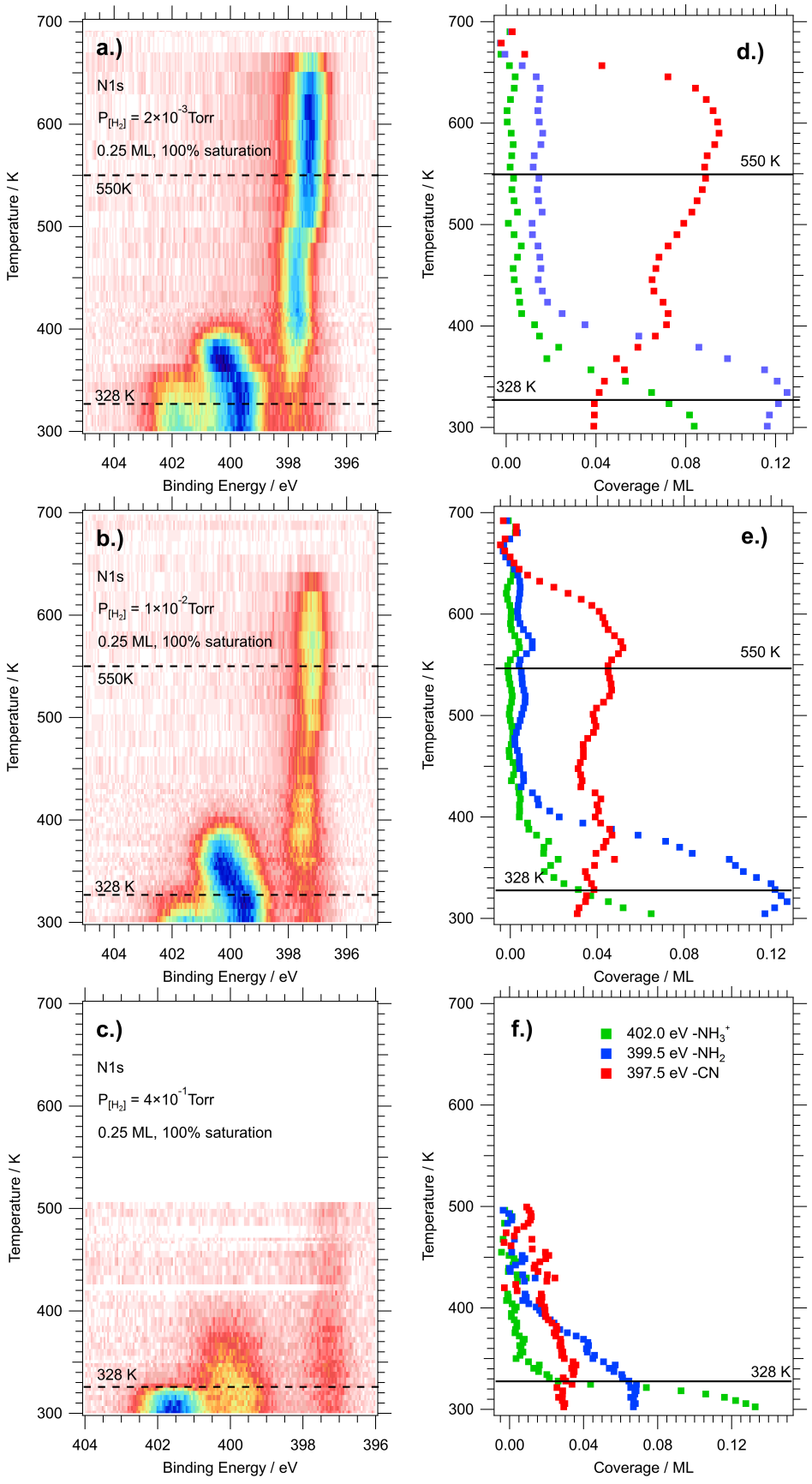
a.)
N1s
P[H2] = 2×10-3Torr
0.25 ML, 100% saturation
550K
328 K
b.)
N1s
P[H2] = 1×10-2Torr
0.25 ML, 100% saturation
550K
328 K
c.)
N1s
P[H2] = 4×10-1Torr
0.25 ML, 100% saturation
328 K
Temperature / K
Binding Energy / eV
d.)
550 K
328 K
e.)
550 K
328 K
f.)
402.0 eV -NH3+
399.5 eV -NH2
397.5 eV -CN
328 K
Coverage / ML

Figure 4: a. - c.: N 1s TP-XPS data recorded for 0.25 ML of alanine on Ni{111} under varying hydrogen pressure; d. - f.: line profiles showing the temperature dependence of characteristic peaks in 2 eV wide bands. Heating rate $0.1 - 0.2$ K s^{-1}; photon energy 650 eV.

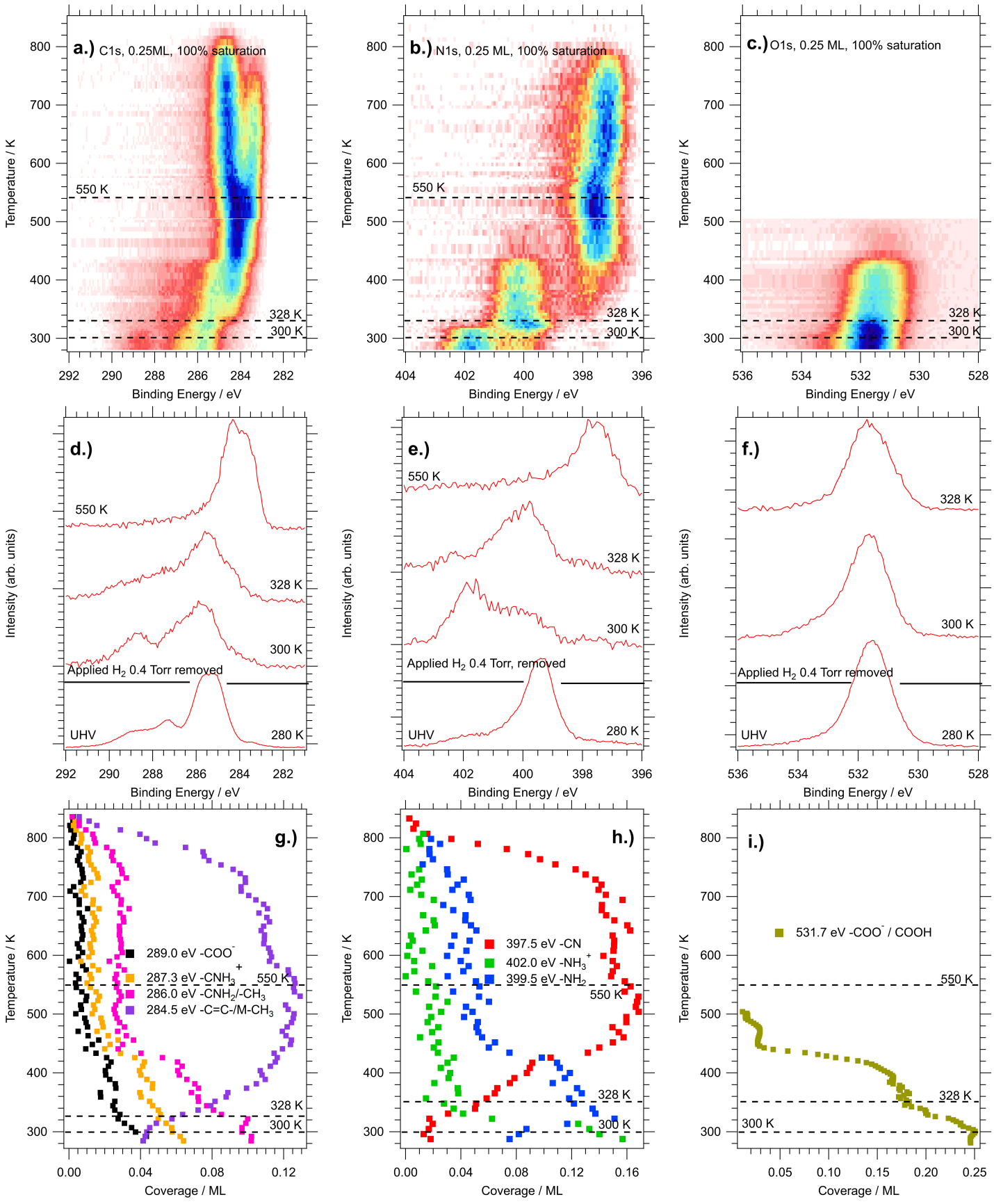
a.) C1s, 0.25ML, 100% saturation
b.) N1s, 0.25 ML, 100% saturation
c.) O1s, 0.25 ML, 100% saturation
Temperature / K
Binding Energy / eV
550 K
328 K
300 K
d.)
e.)
f.)
Intensity (arb. units)
Applied H2 0.4 Torr removed
UHV
280 K
g.)
h.)
i.)
289.0 eV -COO-
287.3 eV -CNH3+
286.0 eV -CNH2/-CH3
284.5 eV -C=C-/M-CH3
397.5 eV -CN
402.0 eV -NH3+
399.5 eV -NH2
531.7 eV -COO- / COOH
Coverage / ML

Figure 5: TP-XPS data recorded for 0.25 ML of alanine adsorbed on Ni{111}. After adsorbtion of a saturated alanine layer, the sample was exposed to 4×10^{-1} Torr of hydrogen for ~ 300 s before the chamber was returned to UHV for the TP-XPS experiment. a.-c.: TP-XPS spectra in the C 1s, N 1s, O 1s regions; d. - f.: individual spectra at key temperatures; g. - i.: line profiles showing the temperature dependence of characteristic peaks in 2 eV wide bands (see text for details). Heating rate $0.1 - 0.2$ K s^{-1}; photon energy 650 eV.

Graphical TOC Entry